A Nebular Origin for Chondritic Fine-Grained Phyllosilicates

Fred J. Ciesla *et al.*

Science **299**, 549 (2003);
DOI: 10.1126/science.1079427

stations PLIG and YAIG displays the same symmetries as the theoretical Green tensor (Fig. 3). Moreover, the arrival times of the pulses in the Z/Z, Z/R, R/Z, R/R, and T/T components of the stacked correlations coincide with those of the Rayleigh and Love signals in the Green tensor. This coincidence in arrival time, as well as the clear Rayleigh and Love polarization of the correlation pulses (Fig. 2B), proves that the observed signals are identified as the Rayleigh and Love pulses of the Green tensor and, most important, that the coda correlation technique does indeed retrieve the surface-wave part of the actual Green tensor between the two stations.

To make sure that the pulse is not simply a surface wave that is generated repeatedly at the coast by the conversion of oceanic waves and that propagates in the direction defined by the two stations, we performed the same test with another pair of stations, YAIG and CUIG, oriented in a different azimuth (Fig. 1). The stacked correlation signals also display pulses with arrival times and polarizations close to the Rayleigh and Love modes of the theoretical Green function (fig. S1), excluding the alternative interpretation of induced surface waves.

So far we have not been able to extract either the high-frequency part of the Green function or the body waves. The lack of high frequencies is most probably a result of the absence of high-frequency waves in the late coda because of anelastic absorption, which acts as a low-pass filter. Another explanation could be that the fundamental modes of Rayleigh and Love waves at low frequency are the part of the field with the simplest modal representation. Retrieving the Green function relies on the orthogonality of the set of eigenfunctions that constitutes the total random field. All cross-products vanish in the averaging, assuming a distribution of sources, or scatterers, that spans the whole space. However, the volume where the spatial source averaging is performed is in practice limited by the number of earthquakes and the locations of scatterers. We speculate that only eigenfunctions with amplitudes concentrated in a zone where inhomogeneities are densely distributed can be adequately extracted. This is the case with the Rayleigh and Love waves, the eigenfunctions of which have a limited penetration in the upper part of the crust where the distribution of scatterers is likely to be dense.

We expect to retrieve both the Green function and its time reciprocal if the diffuse field is perfectly random. This could be the case with an isotropic distribution of sources around the stations or in a finite body. Because all earthquakes are located south of both station PLIG and station YAIG, there is a preferential direction of transport of diffuse energy. This results in a better reconstruction of the Green function in one of the time directions. We also considered a couple of stations along the coast (fig. S2A) for which the distribution of epicenters is more symmetric. The wave propagation is much more complex there (*22*) than in central Mexico, but some features of the Green function emerge from the noisy correlation stacks, such as a clear dispersed Love wave that can be seen in the two directions of time (fig. S2B).

Digital seismic networks provide a large number of coda records, which can be used to compute impulse response between perfectly located positions. This new kind of seismogram could help to produce images of the inner Earth structures without the uncertainties of origin time and source location encountered with traditional earthquake data. A similar approach is applicable in other domains where time series of diffuse waves are available.

References and Notes

1. R. L. Weaver, O. I. Lobkis, *Phys. Rev. Lett.* **87**, 134301 (2001).
2. _____, *J. Acoust. Soc. Am.* **110**, 3011 (2001).
3. K. Aki, B. Chouet, *J. Geophys. Res.* **80**, 3322 (1975).
4. K. Aki, *Phys. Earth Planet. Inter.* **21**, 50 (1980).
5. H. Sato, M. Fehler, *Seismic Wave Propagation and Scattering in the Heterogeneous Earth* (Springer-Verlag and American Institute of Physics Press, 1998).
6. R. S. Wu, K. Aki, *Pure Appl. Geophys.* **128**, 49 (1988).
7. I. R. Abubakirov, A. A. Gusev, *Phys. Earth Planet. Inter.* **64**, 52 (1990).
8. M. Hoshiba, *Phys. Earth Planet. Inter.* **67**, 123 (1991).
9. M. Margerin, M. Campillo, N. M. Shapiro, B. van Tiggelen, *Geophys. J. Int.* **138**, 343 (1999).
10. R. Hennino *et al.*, *Phys. Rev. Lett.* **86**, 3447 (2001).
11. R. L. Weaver, *J. Acoust. Soc. Am.* **71**, 1608 (1982).
12. L. A. Apresyan, Y. A. Kravtsov, *Radiation Transfer: Statistical and Wave Aspects* (Gordon and Breach, Amsterdam, 1996).
13. R. L. Weaver, *J. Mech. Phys. Solids* **38**, 55 (1990).
14. L. V. Ryzhik, G. C. Papanicolaou, J. B. Keller, *Wave Motion* **24**, 327 (1996).
15. E. Akkermans, P. E. Wolf, R. Maynard, G. Maret, *J. Phys. France* **49**, 77 (1988).
16. A. Derode, P. Roux, M. Fink, *Phys. Rev. Lett.* **75**, 4206 (1995).
17. C. Dreager, M. Fink, *J. Acoust. Soc. Am.* **105**, 611 (1999).
18. P. Roux, M. Fink, *J. Acoust. Soc. Am.*, in press.
19. Time-reversal experiments of ultrasonic waves in multiple scattering media give similar results with one-bit signals as with complete wave forms. We computed the correlation functions on the entire length of one-bit coda records. The results are very close to correlations of windowed true-amplitude coda records.
20. A. Derode, A. Tourin, M. Fink, *J. Appl. Phys.* **85**, 6343 (1999).
21. M. Campillo *et al.*, *Geofis. Int.* **35**, 361 (1996).
22. N. M. Shapiro, M. Campillo, S. K. Singh, J. Pacheco, *Geophys. Res. Lett.* **25**, 101 (1998).

23. We thank N. Shapiro, J. Pacheco, and S. K. Singh (Instituto de Geofisica, Universidad Nacional Autónoma de México for making the data available and B. van Tiggelen, L. Margerin, A. Derode, E. Larose, R. Weaver, and G. Abers for enlightening discussions.

Supporting Online Material

www.sciencemag.org/cgi/content/full/299/5606/547/DC1

Figs. S1 and S2

18 September 2002; accepted 5 December 2002

A Nebular Origin for Chondritic Fine-Grained Phyllosilicates

Fred J. Ciesla,[1]* Dante S. Lauretta,[1] Barbara A. Cohen,[2] Lon L. Hood[1]

Hydrated minerals occur in accretionary rims around chondrules in CM chondrites. Previous models suggested that these phyllosilicates did not form by gas-solid reactions in the canonical solar nebula. We propose that chondrule-forming shock waves in icy regions of the nebula produced conditions that allowed rapid mineral hydration. The time scales for phyllosilicate formation are similar to the time it takes for a shocked system to cool from the temperature of phyllosilicate stability to that of water ice condensation. This scenario allows for simultaneous formation of chondrules and their fine-grained accretionary rims.

The CM carbonaceous chondrites are of particular interest to planetary science because they are rich in both water and organic molecules, making them prime candidates for the source of Earth's prebiotic material. The majority of their water is contained within phyllosilicates, which typically occur as small (10 to 100 nm) grains within the fine-grained rims (FGRs) around coarse-grained meteoritic components such as chondrules and calcium-aluminum–rich inclusions. FGR textures, specifically the direct contact of hydrous and anhydrous grains, suggest that these rims accreted on their host objects before being incorporated into their final parent bodies (*1*, *2*) (Fig. 1). If the formation of these phyllosilicates took place on the final parent body, more homogeneous hydration would be expected among the grains. In addition to these FGRs, the CM chondrites also contain evi-

[1]Department of Planetary Sciences, Lunar and Planetary Laboratory, University of Arizona, 1629 East University Boulevard, Tucson, AZ 85721, USA. [2]Hawaii Institute of Geophysics and Planetology, University of Hawaii, Honolulu, HI 96822, USA.

*To whom correspondence should be addressed. E-mail: fciesla@lpl.arizona.edu

dence for liquid water–rock interactions on their parent bodies (*3*).

The most abundant phase in these CM FGRs is chrysotile, $Mg_3Si_2O_5(OH)_4$, which occurs as small (<20 nm) crystals with cylindrical or fibrous morphologies. The second most abundant phase is cronstedtite, $(Fe^{+2,+3})_3(Fe^{+3},Si)_2O_5(OH)_4$, which occurs as relatively large platy grains up to 500 nm in length and 100 nm in width. Some cronstedtite is coherently intergrown with tochilinite, $FeS{\cdot}Fe(OH)_2$ (*2*).

Kinetic studies of chrysotile formation suggested that it could not form as the result of gas-solid reactions in the solar nebula (*4*). Therefore, a formation history involving multiple stages of processing has been proposed to explain how phyllosilicates in CM chondrite FGRs formed before being accreted by chondrules and incorporated into the final parent body (*1*). In this model, the phyllosilicates formed by aqueous alteration on a planetesimal that was catastrophically disrupted, causing the minerals to disperse into the nebula. Chondrules and other coarse-grained components encountered this ejecta, which accreted onto their surfaces, forming FGRs. The chondrules and their FGRs then accreted together to form the parent body. This scenario requires that the original planetesimal was uncompacted and was able to stabilize liquid water (*1*).

It has also been suggested that these minerals could have formed in regions of the nebula where the water vapor pressure was locally enhanced and thus where the hydration reactions would have been more rapid (*5*). Shock waves offer a possible mechanism for locally increasing the pressure of the gas in the nebula and are considered to be among the leading candidates for forming chondrules (*6*–*9*). Thus, shock waves could serve as a mechanism for forming both the chondrules in the CM chondrites and the rims that surround them.

We modified the shock wave model of (*9*) to examine the effects of a chondrule-forming shock wave passing through an icy region of the nebula. In addition to silicate particles, water ice is considered as a solid species. Ice is allowed to sublimate at the rate given in (*10*). As the ice sublimates, the water molecules are incorporated into the nebular gas. The water vapor pressure is then calculated as the nebular gas evolves and is used to estimate the time scale for phyllosilicate formation. The silicates and ice particles in this model are initially treated as 1-mm spheres. The silicates have the same heat capacity and emissivity as in (*9*) and are initially suspended at a mass density of $0.005\ \rho_g$, the local mass density of the nebular gas. Each individual chondrule precursor has a mass density of 3.3 g/cm^3, the density of forsterite. Melting of different silicate minerals occurs over a temperature range of roughly 1400 to 1900 K, and thus the latent heat of melting of the silicates is distributed over that range. The number density of ice particles is determined by calculating the total number of water molecules relative to hydrogen molecules ($n_{H_2O} = 5.1 \times 10^{-4}\ n_{H_2}$ for the canonical solar nebula) and then finding the equilibrium water vapor pressure at the initial temperature in the model. We subtract the number of molecules in the vapor phase and then distribute the rest into solid 1-mm spheres. In addition, we consider the dissociation and recombination of hydrogen molecules as described in (*7*).

Studies of water vapor diffusion in the early solar nebula (*11*, *12*) have shown that water molecules are transported from the inner nebula to the snow line [$a_{snow} \sim 5$ astronomical units (AU), migrating inward with time], where they condense to form ice. The inner nebula loses its water in $\sim 10^5$ years, provided that there is no way for the vapor to migrate inward (*12*). This is much shorter than the time between nebular formation and the onset of chondrule formation ($\sim 10^6$ years) (*13*). Therefore, it can be assumed that all of the water vapor in the inner solar nebula diffuses to beyond the snow line during chondrule formation. This increase in water molecule concentration would lead to the formation of more ice particles just beyond the snow line. In addition, the concentration of ice particles at the midplane would grow even greater through gravitational settling (*14*). Other processes, such as turbulent concentration (*15*), could also serve to increase the local concentration of ice particles. Thus, the concentration of water ice at the snow line could range from the canonical solar nebula value to several thousand times larger in some regions (*16*).

We limit our investigation to shock waves that produce chondrules, that is, those that bring the silicate particles up to peak temperatures ranging from 1700 to 2400 K (*17*, *18*) and that produce cooling rates in the range from 10 to 1000 K/hour as the chondrule approaches the assumed solidus (1400 K).

With the use of the resulting water vapor pressure behind the shock front, we used simple collision theory (SCT) (*4*, *5*) to find the time scale for forsterite hydration to serpentine by calculating the frequency with which the water molecules collide with the forsterite grains and the energy distribution of those collisions. When a collision takes place with an energy greater than the activation energy of the reaction, the reaction moves forward. The activation energy used in this study is 70 kJ/mol, which is the same as that used in (*4*, *5*), based on the amount of energy required to convert MgO to $Mg(OH)_2$ brucite. On the basis of experimental studies of forsterite hydration, it has been suggested that this activation energy is too high (*19*, *20*), although these experiments were done under much different conditions than those expected for the solar nebula. We use a value of 70 kJ/mol as a worst-case scenario. If the actual activation energy of this reaction is lower, the hydration reactions would occur much more rapidly.

We present the results of a simulation of a shock wave traveling at 5 km/s through an icy region of the nebula with a temperature of 150 K and a total gas pressure of 1 Pa and where ice is enhanced by a factor of 700 over the canonical solar ratio (*21*) (Fig. 2). The silicate peak temperature is ~1980 K, and they cool from 1600 to 1400 K at a rate of ~20 K/hour. Before encountering the shock front, the solids are warmed by radiation from the hot particles immediately behind the shock. The vaporization of the ice particles due to this radiation

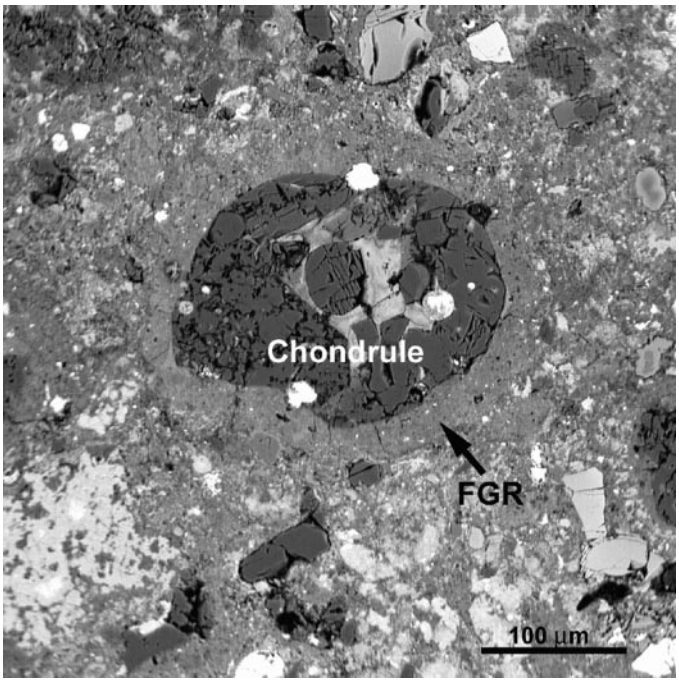

Fig. 1. Back-scattered electron image of a type I chondrule surrounded by a fine-grained, phyllosilicate-rich rim from the Murray CM chondrite. The model presented in this paper is capable of producing the coarse-grained anhydrous silicates and the fine-grained hydrated minerals in the accretionary rim.

results in a nearly five orders of magnitude increase in the partial pressure of the water vapor 15 hours upstream of the shock. As the chondrule precursors are further irradiated, the gas is heated by conduction from the particles, resulting in a gradual increase in total pressure immediately upstream of the shock front. When the gas passes through the shock front, the pressure is increased by a factor of ~40. Interactions with the solids behind the shock front cause an additional increase in pressure, until the relative velocity of the solids with respect to the gas approaches zero. The gas is isobaric as it cools. The hydrogen pressure is 160 Pa, and the water vapor partial pressure is 58 Pa behind the shock. The water vapor would then be available to react with solid materials, particularly those dust particles present, as the system began to cool.

Equilibrium abundances of relevant gaseous and solid phases were calculated for a series of temperature and total pressure values determined from the shock wave model (*22*). At temperatures above 460 K, the only solids that are stable under these conditions are forsterite, fayalite, and enstatite. Troilite becomes stable at 460 K, followed by greenalite at 380 K and chrysotile at 350 K. Water ice condenses at 240 K. We note that Fe metal is not stable under any of the conditions studied here. However, it is likely that many, if not all, metal grains in primitive meteorites originated in chondrule melts, which are decoupled from the surrounding gas phases (*25*, *26*). If metal grains migrated to the exteriors of the chondrule melts, they would quickly react with the gas and begin to oxidize, such that a 100-μm Fe grain would become magnetite in less than 5 hours (*27*). This process explains the absence of metal grains in the exteriors of chondrules in CM chondrites. Tochilinite was not included as one of our solid species because thermodynamic data for this phase are not available, but it would probably form in place of troilite because of the high water vapor pressure.

The increase in the partial pressure of water has two major effects on the formation of phyllosilicates. The rate of phyllosilicate formation increases because it is proportional to the water vapor pressure, which determines the collision rate of water molecules with the surfaces of the grains (*4*, *5*). In addition, the temperature at which phyllosilicates become stable increases. These two factors result in a significant increase in the rate of phyllosilicate formation (Fig. 3).

At 380 K, with an activation energy of 70 kJ/mol, the time scale for a 10-nm grain of fayalite (Fe_2SiO_4) to hydrate to greenalite is 15 hours, or ~0.6 days. At 350 K, the time scale for a 10-nm grain of forsterite to hydrate to chrysotile is 3.8 days. These hydration reactions will proceed as long as there is water vapor to impact the surface of the olivine grains. Thus, once water ice begins to condense, phyllosilicate formation ceases. The time interval between phyllosilicate formation and ice condensation is 12 days (Fig. 4), which is long enough to form 10-nm grains of chrysotile and 100-nm grains of greenalite, the same size as grains observed in chondrule rims in CM chondrites. Thus, our model would produce conditions that would allow for the types and sizes of minerals found in these FGRs to be formed.

Models of aqueous alteration on the CM parent body have shown that the formation of phyllosilicates will cause the internal temperature of the body to rise to 400 K, about 100 K higher than that suggested by the mineralogy (*28*, *29*). If a significant amount of silicate hydration occurred in the nebula, as predicted in our model, then less heat will be produced inside the parent body. The predicted differences between models of the CM asteroid and the mineralogies of the meteorites can thus be reconciled. A sustained lower temperature on aqueously altered parent bodies allows for the survival, and possible delivery to Earth, of organic molecules.

The results of this work are not limited to chondrule formation in regions of the nebula where water ice is drastically enhanced. The level of hydration observed in FGRs may be a result of chondrule and rim formation in regions of the nebula with different ice enhancements. Pre-accretionary hydration of grains in FGRs likely took place for chondrules found in CM, CR, and possibly CI chondrites, whereas those around chondrules in other carbonaceous chondrite groups are largely anhydrous (*30*). Those chondrules with anhydrous rims may simply be the result of shock waves operating in regions of the nebula that were depleted (or at least not

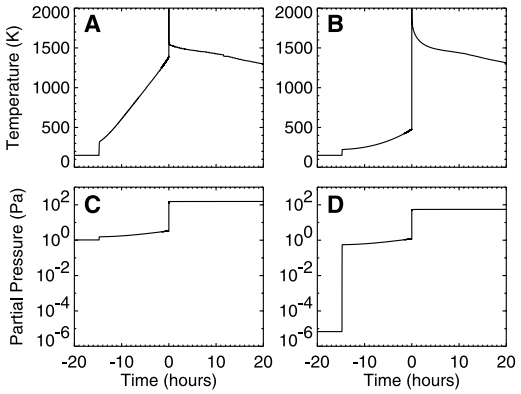

Fig. 2. Thermal and vapor pressure evolution of the shocked system where time $t = 0$ shows where the shock front is encountered. The temperature profiles of (**A**) the silicate particles suspended in the gas and (**B**) the nebular gas are shown, along with the partial pressures of (**C**) hydrogen molecules and (**D**) water vapor. After the shock front passes, the water vapor pressure is increased by nearly seven orders of magnitude, leading to favorable conditions for phyllosilicate formation.

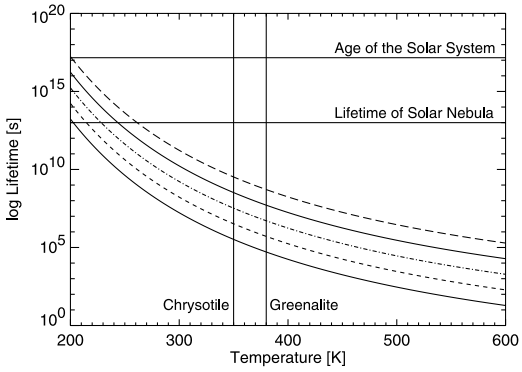

Fig. 3. The time scales for hydration of 10-nm (bottom), 100-nm, 1-μm, 10-μm, and 100-μm (top) olivine grains are plotted as a function of temperature at the water vapor pressure behind the shock wave. The temperature at which the hydration products will be stable depends on the composition of the grains. Greenalite, the iron end-member of serpentine, is stable at 380 K, whereas chrysotile, the magnesium end-member, is stable at 350 K. The expected lifetime of the solar nebula and the age of the solar system are shown for reference.

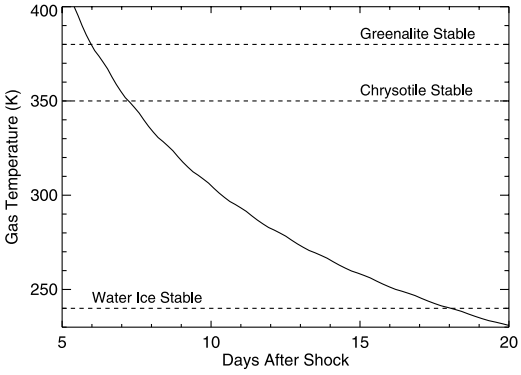

Fig. 4. The cooling profile of the gas after passage of the shock front. The stability temperatures of greenalite, chrysotile, and water ice are 380 K, 350 K, and 240 K, respectively. The shocked system cools to the greenalite stability temperature about 6 days after passing through the shock front; the chrysotile stability temperature is reached one day later, whereas the water ice will begin to condense out 11 days after that. These times are long enough for 10-nm diameter grains of chrysotile and 100-nm grains of greenalite to form.

enhanced) in water vapor. The distribution of water ice throughout the solar nebula may have varied with heliocentric distance and with time (*12*), producing environments with varying rock/water ratios. The existence of extensively hydrated FGRs contained within aqueously altered meteorites implies that the formation of chondrules and eventually meteorite parent bodies may have extended into the region where Jupiter eventually formed.

References and Notes

1. K. Metzler, A. Bischoff, D. Stoffler, *Geochim. Cosmochim. Acta* **56**, 2873 (1992).
2. D. S. Lauretta, X. Hua, P. R. Buseck, *Geochim. Cosmochim. Acta* **64**, 3263 (2000).
3. M. R. Lee, *Meteoritics* **33**, 53 (1993).
4. R. G. Prinn, B. Fegley Jr., *Ann. Rev. Earth Planet. Sci.*, **15**, 171 (1987).
5. B. Fegley Jr., R. G. Prinn, *The Formation and Evolution of Planetary Systems* (Cambridge Univ. Press, Cambridge, 1989), p. 171.
6. H. C. Connolly Jr., S. G. Love, *Science* **280**, 62 (1998).
7. A. Ida, T. Nakamoto, H. Susa, *Icarus* **153**, 430 (2001).
8. S. J. Desch, H. C. Connolly Jr., *Meteorit. Planet. Sci.* **37**, 183 (2002).
9. F. J. Ciesla, L. L. Hood, *Icarus* **158**, 281 (2002).
10. K. D. Supulver, D. N. C. Lin, *Icarus* **146**, 525 (2000).
11. D. J. Stevenson, J. I. Lunine, *Icarus* **75**, 146 (1988).
12. K. E. Cyr, W. D. Sears, J. I. Lunine, *Icarus* **135**, 537 (1998).
13. Y. Amelin, A. N. Krot, I. D. Hutcheon, A. A. Ulyanov, *Science* **297**, 1678 (2002).
14. S. J. Weidenschilling, *Meteorites and the Early Solar System* (Univ. of Arizona Press, Tucson, AZ, 1988), p. 348. The time scale for settling to the midplane for 1-mm ice particles for conditions considered here is ~104 years, much less than the time periods considered.
15. J. N. Cuzzi, R. C. Hogan, J. M. Paque, A. R. Dobrovolskis, *Astrophys. J.* **546**, 496 (2001).
16. Gravitational settling would create a roughly uniform concentration of particles at some given distance from the sun, whereas models of turbulent concentration predict a variety of concentrations in different regions throughout the nebula. Gravitational settling will lead to concentrations of solids that are a few hundred times greater than that of the canonical solar nebula (*14*). Turbulent concentration models predict that concentrations orders of magnitude larger are possible (*15*). It should be pointed out that neither of these concentration mechanisms have been investigated by including diffusive redistribution of a condensable species like water vapor. Also, our model does not require that an entire region of the nebula be enhanced with water ice, but rather only relatively small regions (~ a few hundred km). Significant enhancements of solids such as water ice certainly existed during the early planetesimal building stage (*14*).
17. R. H. Hewins, H. C. Connolly Jr., *Chondrules and the Protoplanetary Disk* (Cambridge Univ. Press, Cambridge, 1996), p. 197.
18. H. C. Connolly Jr., B. D. Jones, R. H. Hewins, *Geochim. Cosmochim. Acta*, **62**, 2725 (1998).
19. W. W. Wegner, W. G. Ernst, *Am. J. Sci. Ser. A* **283**, 151 (1983).
20. D. W. G. Sears, G. D. Akridge, *Meteorit. Planet. Sci.* **33**, 1157 (1998).
21. Such conditions could be reached in a variety of ways. In addition to the enhancement mechanisms mentioned above, radial drift of ice particles from the snow line may have enhanced water ice in the solar nebula from 3 to 5 AU (*12*). If the processing described in this report occured in a warmer region of the nebula, the time that the system would take to cool through the temperature range of interest would be longer than that for the case considered here.
22. Thermodynamic equilibrium calculations were performed with the use of the equilibrium module in the HSC Chemistry v5.0 software package, produced by Outokumpu Research Oy (Pori, Finland). This module calculates multicomponent equilibrium compositions in heterogeneous systems with the use of a database of over 15,000 compounds and a Gibbs energy minimization equilibrium solver. The system is composed of H, He, C, N, O, Mg, Si, S, and Fe. The abundances of all elements except H and O are set at solar system abundances (*23*). The abundances of H and O are enhanced consistent with an ice abundance of 700× solar. The species considered in the calculations included 127 different gaseous molecules as well as Fe metal, forsterite, fayalite, enstatite, ferrosilite, troilite, chrysotile, greenalite, wustite, magnetite, hematite, brucite, Fe(II) hydroxide, Fe(III) hydroxide, graphite, SiC, cohenite, siderite, magnesite, sinoite, and water ice. Thermodynamic data for cronstedtite, the most abundant Fe-bearing phase in phyllosilicate-rich accretionary rims, are not available. However, a thermodynamic model for greenalite, a mineral similar in composition and structure to cronstedtite, was recently developed (*24*), and we use this phase to represent Fe-bearing phyllosilicate material. Thermodynamic data for all other species are included in the software database.
23. K. Lodders, B. Fegley, *The Planetary Scientist's Companion*, 80 (Oxford Univ. Press, New York, 1998), p. 80.
24. M. G. Rasmussen, B. W. Evans, S. M. Kuehner, *Can. Mineral.* **36**, 147 (1998).
25. H. C. Connolly Jr. *et al.*, *Nature* **371**, 136 (1994).
26. D. S. Lauretta, P. R. Buseck, T. J. Zega, *Geochim. Cosmochim. Acta* **65**, 1337 (2001).
27. This reaction time was calculated as the amount of time it would take for an iron grain to react with water vapor to form magnetite using the data from (*4*). Magnetite becomes stable in a system of just H, He, C, N, O, S, and Fe at ~1500 K. Thus, if an iron grain is expelled from the chondrule melt, it will start to form magnetite as the system cooled below this temperature. To be conservative, the time scale here was calculated at 1000 K. The reaction would be much more rapid at the higher temperatures, though the system may cool rapidly at these temperatures.
28. R. E. Grimm, H. Y. McSween Jr., *Icarus* **82**, 244 (1989).
29. B. A. Cohen, R. F. Coker, *Icarus* **145**, 369 (2000).
30. A. Bischoff, *Meteorit. Planet. Sci.* **33**, 1133 (1998).

31. The authors thank H. Connolly, J. Nuth, and two anonymous reviewers for useful discussions and comments and M. Pasek for help in carrying out the equilibrium calculations. Supported by a grant from the NASA Origins program. This is Hawaii Institute of Geophysics and Planetology publication no. 1253 and School of Ocean and Earth Science Technology publication no. 6076.

15 October 2002; accepted 13 December 2002

Robust Normal Mode Constraints on Inner-Core Anisotropy from Model Space Search

Caroline Beghein,* Jeannot Trampert

A technique for searching full model space that was applied to measurements of anomalously split normal modes showed a robust pattern of *P*-wave and *S*-wave anisotropy in the inner core. The parameter describing *P*-wave anisotropy changes sign around a radius of 400 kilometers, whereas *S*-wave anisotropy is small in the upper two-thirds of the inner core and becomes negative at greater depths. Our results agree with observed travel-time anomalies of rays traveling at epicentral distances varying from 150° to 180°. The models may be explained by progressively tilted hexagonal close-packed iron in the upper half of the inner core and could suggest a different iron phase in the center.

The concept of inner-core anisotropy is generally accepted as an explanation for the directional dependence of PKIKP travel times and the anomalous splitting of core-sensitive free oscillations (*1*, *2*). Several models have tried to explain both kinds of data, but amplitude and depth dependence of the anisotropy are still a matter of debate (*1*–*7*). In particular, models derived from the inversion of normal mode data cannot explain the large travel-time anomalies observed for body waves traveling at high epicentral distances (*8*–*10*). Even joint inversions of normal mode and travel-time data fail to reconcile all observations (*4*, *5*, *11*). Outer-core structure was even suggested to explain all existing data but could not account for the strong splitting of modes highly sensitive to inner-core structure (*6*). The inner core is believed to be mainly composed of solid iron, with some unknown light elements (*12*–*16*). Although the stable phase of iron at inner-core conditions is not known, mineralogical studies tend to favor a hexagonal close-packed (h.c.p.) structure. Nevertheless, the possibility of another stable phase is not excluded, especially in the presence of lighter elements (*15*). Estimates of the elastic properties of h.c.p. iron at high pressure and temperature (*17*) suggest that the basal plane of one-third of the crystals would have to be aligned with Earth's spin axis to match travel-time observations.

The inner core is generally modeled as a cylindrical medium with a symmetry axis parallel to Earth's rotation axis (*1*, *2*). In that case, normal mode theory (*18*) shows that zonal structure coefficients at degrees two and four are linearly related to three parameters that describe seismic anisotropy:

Faculty of Earth Sciences, Utrecht University, Post Office Box 80021, 3508 TA Utrecht, Netherlands.

*To whom correspondence should be addressed. E-mail: beghein@geo.uu.nl